Mon. Not. R. Astron. Soc. **000**, 000–000 (0000) Printed 25 June 1999 (MN LaTeX style file v1.4)

Microwave polarization in the direction of galaxy clusters induced by the CMB quadrupole anisotropy

S. Y. Sazonov[1,2] and R. A. Sunyaev[1,2]
[1] *MPI für Astrophysik, Karl-Schwarzschild-Str. 1, 86740 Garching bei München, Germany*
[2] *Space Research Institute (IKI), Profsoyuznaya 84/32, Moscow 117810, Russia*

25 June 1999

ABSTRACT

Electron scattering induces a polarization in the cosmic microwave background (CMB) signal measured in the direction of a galaxy cluster due to the presence of a quadrupole component in the CMB temperature distribution. Measuring the polarization towards distant clusters provides the unique opportunity to observe the evolution of the CMB quadrupole at moderate redshifts, $z \sim 0.5$–3. We demonstrate that for the local cluster population the polarization degree will depend on the cluster celestial position. There are two extended regions in the sky, which are opposite to each other, where the polarization is maximal, $\sim 0.1(\tau/0.02)\,\mu$K in the Rayleigh-Jeans part of the CMB spectrum (τ being the Thomson optical depth across the cluster). This value exceeds the polarization introduced by the cluster transverse peculiar motion if $v_t < 1300$ km/s. One can hope to detect this small signal by measuring a large number of clusters, thereby effectively removing the systematic contribution from other polarization components produced in clusters. These polarization effects, which are of the order of $(v_t/c)^2\tau$, $(v_t/c)\tau^2$ and $(kT_e/m_ec^2)\tau^2$, as well as the polarization due to the CMB quadrupole, were previously given by Sunyaev and Zel'dovich for the Rayleigh-Jeans part of the spectrum. We fully confirm their earlier results and present exact frequency dependencies for all these effects. The polarization degree is considerably higher in the Wien region.

Key words: cosmic microwave background – cosmology: theory – galaxies: clusters: general – polarization.

1 INTRODUCTION

The intensity of the cosmic microwave background radiation is distorted in the direction of galaxy clusters. There are two basic effects of this kind: the thermal effect (Sunyaev & Zel'dovich 1972) and the kinematic effect (Sunyaev & Zel'dovich 1980). The polarization of the CMB should be changed due to the presence of galaxy clusters along the line of sight as well (Sunyaev & Zel'dovich 1980; Zel'dovich & Sunyaev 1980; Sunyaev & Zel'dovich 1981). In fact there are several separate polarization effects but since the expected amplitude of each of them is very small, until recently there was little interest to them. However, we have observed such a significant progress in CMB measurements over the period passed since 1980, that the possibilty to detect a CMB-induced polarization signal from galaxy clusters seems no longer unrealistic. Furthermore, the CMB experiments planned for the next decade, which include the space missions MAP (http://map.gsfc.nasa.gov), SPOrt on the International Space Station (Cortiglioni et al. 1998), and Planck Surveyor (http://astro.estec.esa.nl/Planck; De Zotti et al. 1999); and a number of ground-based and baloon-borne experiments, e.g. POLAR (Keating et al. 1998), will already reach a level of sensitivity which is not far from what is needed for such a detection. This drastic change in the situation is reflected in the fact that several new papers (Audit & Simmons 1999; Itoh, Nozawa & Kohyama 1998; Hansen & Lilje 1999) discussing the polarization effects in clusters have appeared over the past year or so. Some authors (Audit & Simmons 1999; Itoh et al. 1998) have claimed the necessity to revise the original results of Sunyaev & Zel'dovich (1980). This gave us a first motivation to return to this problem.

Another reason for us to begin this study was the discovery by COBE (see, e.g. Kogut et al. 1996) of a quadrupole component in the CMB angular anisotropy. Zel'dovich & Sunyaev (1980) showed that the presence of a quadrupole component should cause a change in the CMB polarization in the direction of a galaxy cluster. Already our first estimate based on the COBE measurement lead us to the rather surprising conclusion that this polarization effect should generally be stronger than any of the other polarization effects relating to galaxy clusters. This fact makes the quadrupole-

© 0000 RAS

induced polarization potentially very important for cosmology. Indeed, measuring the microwave polarization signal towards distant galaxy clusters opens the unique opportunity to effectively probe the CMB quadrupole anisotropies at intermediate redshifts, $z \sim 0.5$–3, i.e. from positions in the Universe different from ours, thus giving us a way to reduce the cosmic-variance uncertainty (Kamionkowski & Loeb 1997). Furthermore, by observing the effect in clusters (or any large-scale ionized gas clouds) at large z we could be able to follow the evolution of the CMB quadrupole, which should be different for universes with different cosmological parameters.

The structure of the paper is as follows. In Section 2 we give the basic formulae which allow one to find the angular distribution of the polarized radiation resulted from scattering of a given initial angular distribution of unpolarized radiation by a single resting electron. In Section 3 we calculate the amplitude and distribution over the sky of the polarization imposed by the CMB quadrupole on the signal from clusters. We study other polarization effects connected with galaxy clusters in Section 4, which is followed by a Discussion of possibilities to detect the cluster polarization due to the CMB quadrupole.

2 POLARIZATION DUE TO SCATTERING OF ANISOTROPIC RADIATION BY A SINGLE ELECTRON

In this section, which lays the basis for our further analysis, we basically repeat the original treatment of Zel'dovich & Sunyaev (1980), which is also described in detail in a review paper of Sunyaev & Zel'dovich (1981).

We consider the situation that a single electron being at rest scatters initially unpolarized radiation. The frequency of a photon does not change due to scattering (one can safely neglect the small change due to recoil when dealing with the CMB), and we therefore can, for the moment, ignore the spectral dependence of the radiation and consider only its angular distribution. This distribution can, in general, be presented as the sum of components proportional to the Legendre polynomials $P_n(\mu)$: 1, μ, $(\mu^2-1/3)$, etc., where μ is the cosine of the angles between the wave vector of the incident photon and one of a set of directions that uniquely define our particular angular distribution. The incident radiation is described by a usual set of Stokes parameters, (I, Q, U, V), where $Q=U=V=0$. Our aim is to determine the corresponding quantities (to be marked with primes) for the scattered radiation. The fourth Stokes parameter, V, describes circular polarization which is not produced in a scattering and will, therefore, not be mentioned further. We define the Stokes parameters of the scattered radiation with respect to a reference plane which contains a) the specific direction about which a given radiation anisotropy component has an axial symmetry (see above), and b) the wave vector of the scattered photon. The Q parameter characterizes the linear polarization either in this plane ($Q<0$) or perpendicular to it ($Q>0$). The U parameter describes the linear polarization in the two orthogonal planes inclined at an angle of $\pm\pi/4$ to the reference plane. With this choice of the Stokes parameters, it is easy to show (Chandrasekhar 1950; Sunyaev & Zel'dovich 1981) that the scattered radiation will be

$$I'(\mu') = \int_{-1}^{1}\left[\frac{1}{2}+\frac{3}{16}(3\mu'^2-1)\left(\mu^2-\frac{1}{3}\right)\right]I(\mu)\,d\mu, \tag{1}$$

$$Q'(\mu') = \int_{-1}^{1}\frac{9}{16}(1-\mu'^2)\left(\mu^2-\frac{1}{3}\right)I(\mu)\,d\mu,\;\; U'(\mu')=0. \tag{2}$$

One can see that the angular scattering function for the Q Stokes parameter is of strictly quadrupole form (with respect to μ). This fact is of importance for our further consideration, because it means that, due to the orthogonality condition for Legendre polynomials, only the quadrupole component, neither the dipole nor the higher harmonics, in the incident intensity distribution will contribute to Q'.

Now let the isotropic and multipole components of the intensity distribution be I_0, $I_1\mu$, $I_2(\mu^2-1/3)$, etc. Then upon integration in (1)–(2) we derive

$$I'(\mu') = I_0+\frac{1}{10}I_2\left(\mu'^2-\frac{1}{3}\right), \tag{3}$$

$$Q'(\mu') = \frac{1}{10}I_2(1-\mu'^2),\;\; U'(\mu')=0. \tag{4}$$

As expected, the isotropic component remains unchanged upon scattering. If one now considers a situation that the optical depth of the scattering medium is very small, $\tau \ll 1$, then only single scatterings of photons will play role, and it is straightforward to modify formulae (3), (4), which were obtained for an individual electron, for this case:

$$\begin{aligned} I'(\mu') &= I(\mu')(1-\tau)+\tau\left[I_0+\frac{1}{10}I_2\left(\mu'^2-\frac{1}{3}\right)\right] \\ &= I(\mu')-\tau\left[I_1\mu'+0.9I_2\left(\mu'^2-\frac{1}{3}\right)+\sum_{n=3}^{\infty}I_nP_n(\mu')\right], \end{aligned} \tag{5}$$

$$Q'(\mu') = \frac{1}{10}\tau I_2(1-\mu'^2),\;\; U'(\mu')=0. \tag{6}$$

Equations (5), (6) show that electron scattering tends to smooth anisotropies in the intensity distribution and to produce a polarization on the order of $Q'/I' = 0.1\tau I_2/I_0(1-\mu'^2)$ (Zel'dovich & Sunyaev 1980; Sunyaev & Zel'dovich 1981).

3 POLARIZATION DUE TO THE CMB QUADRUPOLE

The COBE satellite provided the first measurement of the quadrupole component in the CMB angular distribution. Although the accuracy of this measurement is very low – its amplitude, Q_{rms}, is said to lie in the range $[4,28]$ μK at 95% confidence (Kogut et al. 1996) – it is very likely that the detection of the quadrupole is real, because the presence of a similar quadrupole signal, $Q_{rms-ps} \sim 15\mu$K, also follows from the extrapolation of the CMB power spectrum from higher multipole moments to $l=2$ (Bennett et al. 1996).

The CMB quadrupole should cause the microwave radiation from clusters of galaxies to be polarized. Below we present a formalism that allows one to calculate the quadrupole-induced polarization to be measured from a cluster with given celestial coordinates for a given CMB quadrupole. Rather as an example (because of the large uncertainty present) we find the distribution of the polarization signal over the sky as implied by the COBE measurement. It will be straightforward to update our current, rough estimates as new, more accurate measurements (the first of this kind is likely to be provided by MAP) become available. Although, the formulae below are directly applicable only for clusters which belong to the local population, i.e. for measuring the quadrupole that is observed at the current epoch from Earth, one can easily extend our approach on the determination of quadrupoles as seen from highly redshifted clusters.

The COBE quadrupole is defined by 5 parameters, which are essentially coefficients at spherical second-order harmonics (Kogut et al. 1996): $Q_1 = (19.0 \pm 7.4 \pm 8.2)$ μK, $Q_2 = (2.1 \pm 2.5 \pm 2.7)$ μK, $Q_3 = (8.9 \pm 2.0 \pm 2.5)$ μK, $Q_4 = (-10.4 \pm 8.0 \pm 4.3)$ μK, and $Q_5 = (11.7 \pm 7.3 \pm 10.4)$ μK. Here, the first quoted errors are statistical, which are followed by the COBE team's estimates of the present systematic errors. One can construct from the Q_i parameters a tensor $Q_{\alpha\beta}$ with the following components

$$Q_{xx} = Q_4 - \frac{1}{2}Q_1, \;\; Q_{yy} = -Q_4 - \frac{1}{2}Q_1, \;\; Q_{zz} = Q_1,$$
$$Q_{xy} = Q_{yx} = Q_5, \;\; Q_{xz} = Q_{zx} = Q_2, \;\; Q_{yz} = Q_{zy} = Q_3. \quad (7)$$

The quadrupole signal, I_Q, can be calculated for any direction as $I_Q = \sum Q_{\alpha\beta} r_\alpha r_\beta$, where the Cartesian coordinates r_α are expressed through the Galactic coordinates l and b, i.e. $X = \cos l \cos b$, $Y = \sin l \cos b$, and $Z = \sin b$. The $Q_{\alpha\beta}$ tensor possesses the property $Q_{xx} + Q_{yy} + Q_{zz} = 0$.

We can next find the eigenvalues λ_1, λ_2, λ_3 (let λ_1 be the minimum and λ_2 the maximum among the three λ_i) and the corresponding eigenvectors $\vec{e_1}$, $\vec{e_2}$, $\vec{e_3}$ for the $Q_{\alpha\beta}$ tensor in a usual way: $Q_{\alpha\beta}\vec{e_i} = \lambda_i \vec{e_i}$. On introducing spherical coordinates, θ and ϕ (with the polar angle θ measured from $\vec{e_3}$), we can, using the property $\lambda_1 + \lambda_2 + \lambda_3 = 0$, cast the quadrupole signal in a simple form:

$$\begin{aligned} I_Q &= \lambda_1 \sin^2\theta \cos^2\phi + \lambda_2 \sin^2\theta \sin^2\phi + \lambda_3 \cos^2\theta \\ &= \lambda_x \left(\sin^2\theta\cos^2\phi - \frac{1}{3}\right) + \lambda_y \left(\sin^2\theta \sin^2\phi - \frac{1}{3}\right), \end{aligned} \quad (8)$$

where $\lambda_x = \lambda_1 - \lambda_3$ and $\lambda_y = \lambda_2 - \lambda_3$. The RMS amplitude of the quadrupole signal is given by

$$Q_{rms}^2 = \frac{4}{45}(\lambda_x^2 - \lambda_x\lambda_y + \lambda_y^2). \quad (9)$$

For the COBE specific values (as we use these only for illustration purposes, we will quote no errors for the numbers to follow), we find $\lambda_1 = -25$ μK (minimum), $\lambda_2 = 23$ μK (maximum), $\lambda_3 = 2$ μK, $\lambda_x = -27$ μK, $\lambda_y = 22$ μK. The RMS amplitude $Q_{rms} = 12.6$ μK. Note that this value was calculated here without taking account of the existing correlation between the signal and noise in the COBE data, the inclusion of which would have given a slightly lower value (10.7 μK), as explained in (Kogut et al. 1996). The principal vectors $\vec{e_1}$, $\vec{e_2}$, $\vec{e_3}$ point to the following positions in the sky (l, b): (335°, 2°), (250°, -63°), (64°, -27°).

We have thus expressed the quadrupole signal as the sum of two orthogonal components proportional to the Legendre polinomial of second order, one of which is defined with respect to the minimum direction of the CMB quadrupole ($\pm\vec{e_1}$) and the other with respect to its maximum direction ($\pm\vec{e_2}$). We can therefore take advantage of formulae (5) and (6) of Section 2. Although those equations were originally thought of in intensity terms, we can carry out our further analysis in terms of the brightness temperature by introducing temperature Stokes parameters, (T, Q_T, U_T), bearing in mind that small changes in temperature parameters, e.g. $\Delta Q_T/T$, are related to the corresponding changes in intensity parameters, i.e. $\Delta Q_\nu / I_\nu$, via the frequency function

$$f(x) = \frac{d\ln I_\nu}{d\ln T} = \frac{xe^x}{e^x - 1}, \quad (10)$$

where $x = h\nu/kT$ is a dimensionless frequency. Since the change in the CMB in the direction of a galaxy cluster is very small, the resulting polarization degree will obviously have a frequency dependence defined by formula (10), $P'(x) = f(x)(Q_T'^2 + U_T'^2)^{1/2}/T$.

Let $T(\theta, \phi)$ be the initial CMB temperature distribution in which the main isotropic component $T_0 = 2.73$ K, and $T_1\mu$ and $T_n P_n(\mu)$ are the dipole and multipole ($n \geq 3$) harmonics. The temparature distortion in the direction (θ, ϕ) of a cluster can be found directly from equation (5):

$$\begin{aligned} T'(\theta,\phi) = T(\theta,\phi) - \tau \Big\{ T_1\mu + 0.9 \Big[\lambda_x \left(\sin^2\theta\cos^2\phi - \frac{1}{3}\right) \\ + \lambda_y \left(\sin^2\theta\sin^2\phi - \frac{1}{3}\right)\Big] + \sum_{n=3}^{\infty} T_n P_n(\mu) \Big\}. \end{aligned} \quad (11)$$

Equation (6) enables finding the emergent polarization introduced by each of the two orthogonal quadrupole components of the incident temperature distribution. The resulting two sets of Stokes parameters will, however, be measured with respect to different coordinate basises: the one corresponding to the λ_x quadrupole is defined relative to the viewing direction (θ, ϕ) and the $\vec{e_1}$ vector, while the one corresponding to the λ_y quadrupole relative to the viewing direction and the $\vec{e_2}$ vector. In order to find the net signal (Q_T', U_T'), we first need to convert the individual polarization signals, Q_{Tx}' and Q_{Ty}' ($U_{Tx}' = U_{Ty}' = 0$), to common axis, which we set here based on the plane that contains the viewing direction and the $\vec{e_3}$ vector (so that if $Q_T > 0$ and $U_T = 0$, then the vector of polarization is orthogonal to $\vec{e_3}$) and then find the sum of the transformed Stokes parameters (see, e.g. Chandrasekhar 1950):

$$\begin{aligned} Q_T'(\theta,\phi) &= Q_{Tx}'(\theta,\phi)\cos 2\alpha_x + Q_{Ty}'(\theta,\phi)\cos 2\alpha_y, \\ U_T'(\theta,\phi) &= Q_{Tx}'(\theta,\phi)\sin 2\alpha_x + Q_{Ty}'(\theta,\phi)\sin 2\alpha_y. \end{aligned} \quad (12)$$

Here the rotation angles α_x and α_y are given by

$$\begin{aligned} \cos\alpha_x &= -\cos\theta\cos\phi(1 - \sin^2\theta\cos^2\phi)^{-1/2}, \\ \cos\alpha_y &= -\cos\theta\sin\phi(1 - \sin^2\theta\sin^2\phi)^{-1/2}. \end{aligned} \quad (13)$$

We finally get

$$\begin{aligned} Q_T'(\theta,\phi) = 0.1\tau[\lambda_x(\cos^2\theta\cos^2\phi - \sin^2\phi) \\ + \lambda_y(\cos^2\theta\sin^2\phi - \cos^2\phi)], \end{aligned} \quad (14)$$

$$U_T'(\theta,\phi) = 0.1\tau(\lambda_x - \lambda_y)\cos\theta\sin 2\phi, \quad (15)$$

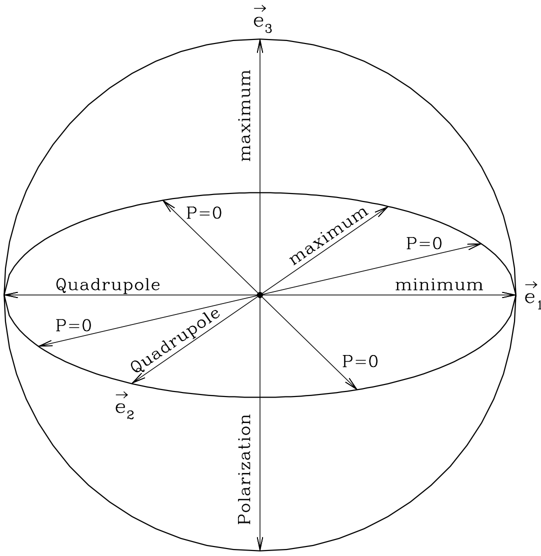

Figure 1. The geometry of the polarization effect induced by the CMB quadrupole. The vectors $\vec{e_1}$, $\vec{e_2}$ and $\vec{e_3}$ define the eigensystem of the CMB quadrupole temperature anisotropy. The polarization effect has two broad maxima in the directions $\pm\vec{e_3}$ orthogonal to the plane which contains the minima ($\pm\vec{e_1}$) and maxima ($\pm\vec{e_2}$) of the quadrupole. In the same plane there are four directions for which there is no polarization.

$$P'(\theta,\phi,x)=0.1f(x)\tau T_0^{-1}\left\{\left[\lambda_x(1-\sin^2\theta\cos^2\phi)\right.\right.$$
$$\left.\left.+\lambda_y(1-\sin^2\theta\sin^2\phi)\right]^2-4\lambda_x\lambda_y\cos^2\theta\right\}^{1/2}. \qquad (16)$$

The polarization degree depends on the cluster position on the celestial sphere in accordance with formula (16). The angular dependence has two maxima, $P_{max}=0.1f(x)\tau T_0^{-1}(\lambda_y-\lambda_x)$, in opposite directions, $\pm\vec{e_3}$. The maximal polarization signal expressed in absolute units is $0.1(\lambda_y-\lambda_x)\tau=4.9\tau$ μK. In the directions of the minima and maxima of the CMB quadrupole, $\pm\vec{e_1}$ and $\pm\vec{e_2}$, $P=0.1f(x)\tau T_0^{-1}\lambda_y$ and $0.1f(x)\tau T_0^{-1}|\lambda_x|$, respectively, and these four positions are saddle points in which the polarization is maximal in the plane $\theta=\pi/2$ and minimal in the perpendicular direction. There are also four positions in the same $\theta=\pi/2$ plane for which $P=0$: $\phi=\pm\arctan\,(-\lambda_y/\lambda_x)^{1/2}$ and $\phi=\pi\pm\arctan\,(-\lambda_y/\lambda_x)^{1/2}$. The geometry of the effect is sketched in Fig. 1.

The sky-average (RMS) polarization induced by the CMB quadrupole can be found from expression (16) to be

$$P_{rms}(x)=0.1f(x)\tau T_0^{-1}\sqrt{\frac{8}{15}(\lambda_x^2-\lambda_x\lambda_y+\lambda_y^2)}, \qquad (17)$$

or, using equation (9),

$$P_{rms}(x)=\frac{\sqrt{6}}{10}f(x)\tau\frac{Q_{rms}}{T_0}. \qquad (18)$$

Note the $\sqrt{6}$ enhancement factor in this relation. For the COBE data the sky-average polarization is 3.1τ μK, or 0.6 of the maximal signal.

Expanding expression (16) in the vicinity of the maximum directions, $\theta=0$, π, gives

$$\frac{\Delta P}{P_{max}}=\frac{\lambda_x\cos^2\phi-\lambda_y\sin^2\phi}{\lambda_y-\lambda_x}(\Delta\theta)^2. \qquad (19)$$

The quadratic dependence on the angular shift implies that the polarization maxima are very broad. Each of the two roughly elliptical areas around the maxima within which $P/P_{max}>1/2$ subtends about a quarter of the sky, as implied by the COBE measurement. Obviously, in these extended regions one has best chances to detect the quadrupole-induced polarizion. We note, however, that the measurement of the effect in the direction of its maxima is not sufficient for deducing all the 5 parameters that define the global quadrupole, so measurements in other directions are still necessary.

In contrast to the maxima, the four directions in which there is no polarization signal are well resolved, as near them

$$\frac{P}{P_{max}}=2\frac{\sqrt{-\lambda_x\lambda_y}}{\lambda_y-\lambda_x}\sqrt{(\Delta\phi)^2+(\Delta\theta)^2}. \qquad (20)$$

The minima are sharp because the Stokes parameters Q and U change their sign in these points. The area around a minimum within which $P/P_{max}<1/4$ is a 14° radius circle for the adopted COBE values.

The polarization caused by the CMB quadrupole is very small, reaching at the maximum $P_{max}\sim 2\cdot 10^{-6}f(x)\tau$ or, equivalently, $0.1(\tau/0.02)$ μK. This fact does not, however, automatically require the detector sensitivity threshold be accordingly low. Instead, one can derive the polarization corresponding to a given direction by averaging polarization signals taken from a large number of clusters located roughly around this direction (to be more precise, two opposite directions can be probed at the same time). In such a study, it is, in principle, even not necessary to have information on the optical depth of each particular cluster. Indeed, the polarization effect depends linearly on τ, therefore it is the ensemble-average optical depth which is important. Furthermore, all other possible polarization effects associated with clusters, which we discuss below, are not additive, in contrast to the quadrupole effect, i.e. summing up signals from individual clusters will tend to smooth out their contribution.

4 OTHER POLARIZATION MECHANISMS IN CLUSTERS OF GALAXIES

4.1 Polarization due to cluster transverse motion

Sunyaev & Zel'dovich (1980) have shown that the proper motion of a galaxy cluster relative to the CMB will induce a polarization in the microwave signal measured from the cluster. They calculated this effect for the Rayleigh-Jeans region of the CMB spectrum and indicated (see formula (8) in their 1980 paper) how to calculate the effect for any desired frequency. We now intend to find the frequency dependence of the produced polarization in explicit form.

Let us assume that the initial microwave background is isotropic and has a black-body spectrum of temperature

T_0. Now let an electron move through this background at a speed v. In the electron's rest frame, the radiation spectrum is also black-body, but with a temperature depending on the viewing direction. The spectral intensity in this frame is given by

$$I_\nu = C\frac{x^3}{e^{x\gamma(1+\beta\mu)}-1}, \tag{21}$$

where $C = 2(kT_0)^3/(hc)^2$, $\beta = v/c$, $\gamma = (1-\beta^2)^{-1/2}$, μ is the cosine of the angle between the electron's velocity vector and the direction of incidence of a photon, and all the quantities are measured in the rest frame of the electron. The angular distribution of the background can be expanded in Legendre polynomials. Retaining only terms up to the second order in β^2, one gets

$$I_\nu = C\frac{x^3}{e^{x\gamma}-1}\left[\left(1+\frac{e^x(e^x+1)}{6(e^x-1)^2}x^2\beta^2\right)-\frac{e^x}{e^x-1}x\beta\mu \right.$$
$$\left. +\frac{e^x(e^x+1)}{2(e^x-1)^2}x^2\beta^2\left(\mu^2-\frac{1}{3}\right)+...\right]. \tag{22}$$

Thus the quadrupole component of the initial distribution is

$$\frac{I_2}{I_0} = \frac{e^x(e^x+1)}{2(e^x-1)^2}x^2\beta^2. \tag{23}$$

In the limit $x \to 0$, corresponding to the Rayleigh-Jeans spectral region, $I_2/I_0 = \beta^2$. In the opposite limit, $x \to \infty$, one has $I_2/I_0 = 1/2x^2\beta^2$. The transformation of the resulting polarization to the CMB frame will produce additional terms which are of higher than the second order in β, so we will ignore them here. Using equations (5) and (6), we then finally obtain the polarization to be measured towards a cluster moving in the direction μ' with respect to the observer,

$$P'_\nu = 0.1\frac{e^x(e^x+1)}{2(e^x-1)^2}x^2\beta_t^2\tau. \tag{24}$$

Here, $\beta_t = \beta(1-\mu'^2)^{1/2}$ is the transverse component of the peculiar velocity of the cluster. The polarization vector is perpendicular to the plane formed by the velocity vector and the observing direction. In the Rayleigh-Jeans frequency region, we readily find $P'_\nu = 0.1\beta_t^2\tau$, exactly the result of Sunyaev & Zel'dovich (1980). In the Wien part of the spectrum ($x \to \infty$), the degree of polarization of the measured signal is much higher, a fact mentioned by Zel'dovich & Sunyaev (1981). Fig. 2(a) shows the distribution of the polarized signal in the plane of the sky for a spherical cluster.

It is easy to show that the frequency-integrated polarization $\int Q'_\nu\, d\nu / \int I'_\nu\, d\nu = \beta_t^2\tau$, in agreement with the result of Audit & Simmons (1999). We note that the result given in equation (24) is different from the one obtained by Itoh et al. (1998).

4.2 Polarization effects due to finite optical depth

Sunyaev & Zel'dovich (1980) have shown that there is another polarization mechanism associated with galaxy clusters which is connected with two consecutive scatterings of a photon within the intracluster gas, i.e. with finite optical depth of the gas cloud. Indeed, after first scattering in the intracluster medium, the CMB acquires an anisotropy due to the thermal and kinematic effects. The magnitude of this local anisotropic component is proportional to the product of τ and $\eta = kT_e/m_ec^2$ for the thermal effect (T_e being the temperature of the plasma) and β for the kinematic effect. Second scattering within the cluster will induce polarization signals of the order of $\eta\tau^2$ and $\beta\tau^2$. In the first approximation, the frequency dependence of the polarization will be the same as that of the thermal or kinematic effect. The resulting distribution of the degree and direction of polarization over the cluster projected on the sky will be determined by the distribution of gas density and temperature within the cluster, on which depends the magnitude of the local quadrupole component.

Before going further we would like to point out that the thermal and kinematic effects are not the only possible mechanisms capable of producing a local anisotropy. The local intensity distribution should also be distorted by gravitational effects, the most important of which is the effect of a moving gravitational lense (connected with the cluster peculiar motion). The resulting polarization was calculated

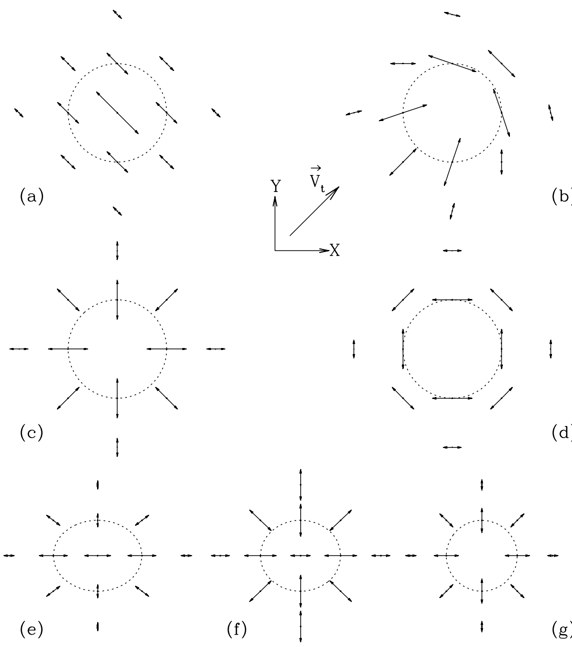

Figure 2. Predicted angular distributions of the polarized signal in the direction of galaxy clusters. In cases (a)–(d) the model gas cloud is spherical and an isothermal density law with $n = 3/2$ is assumed. (a) The polarization $\propto \beta_t^2\tau$ caused by the peculiar motion in the indicated direction (see the insert in the center of the figure). (b) The finite optical depth polarization $\propto \beta_t\tau^2$ for the same peculiar motion. (c) The finite optical depth polarization $\propto (kT_e/m_ec^2)\tau^2$ at frequencies $x < 3.83$. (d) The same but at $x > 3.83$. (e) The gas cloud is a spheroid with the ratio of the principal axes $b/a = 0.8$ and the symmetry (longer) axis in the X direction. (f) The same but the symmetry axis is inclined at 45° to the picture plane. (g) The same but the symmetry axis points along the line of sight. The projected core of the cluster (as defined by the isothermal law) is shown by the dashed lines in all panels.

© 0000 RAS, MNRAS **000**, 000–000

by Gibilisco (1997), and for very massive clusters it can be of comparable magnitude with the effects we discuss.

Sunyaev & Zel'dovich (1980) estimated the finite depth effects for a homogeneous spherical gas cloud. We will first check their results and then consider more realistic models for the gas distribution in clusters. It turned out that the simple formulae obtained in Section 2 are not readily applicable to the problem at hand. We have therefore chosen to follow a more straightforward approach, which is outlined below.

We introduce a coordinate system in which the $\vec{OZ}$ axis is pointed from the cluster in our direction and the picture plane contains the $\vec{OX}$ and $\vec{OY}$ axes. Our task is to calculate the polarization that would be measured from a given (X,Y) projection point. For a given model we must specify a density law, $\rho(X,Y,Z)$, where we, for simplicity, by density mean the number density of electrons. The gas temperature η is assumed constant throughout the cluster in all of our models.

The calculation runs as follows. To the effect from the (X,Y) point contribute all points (X,Y,Z) along the line of sight passing through this projection point. Therefore, one needs to find for each such point the angular intensity distribution (in which the isotropic component can be ignored) resulted from the first scattering, $\Delta I(X,Y,Z,\theta,\phi)$. Here, the θ and ϕ angles define the viewing direction $\vec{l}$: $(\sin\theta\cos\phi, \sin\theta\sin\phi, \cos\theta)$. If we define the Stokes parameters with respect to the $\vec{OX}$ and $\vec{OY}$ axes ($Q>0$, $U=0$ corresponds to a polarization in the $\vec{OY}$ direction), then the resulting polarization will be

$$Q'_\nu(X,Y) = \frac{3\sigma_{\rm T}}{16\pi} \times \int dZ\,\rho(X,Y,Z)\int d\vec{\Omega}\sin^2\theta\cos(2\phi)\Delta I_\nu(X,Y,Z,\theta,\phi) \quad (25)$$

$$U'_\nu(X,Y) = \frac{3\sigma_{\rm T}}{16\pi} \times \int dZ\,\rho(X,Y,Z)\int d\vec{\Omega}\sin^2\theta\sin(2\phi)\Delta I_\nu(X,Y,Z,\theta,\phi), \quad (26)$$

where σ_T is the Thomson scattering cross section.

Equations (25) and (26) take account of the Rayleigh scattering function and of the fact that the polarization vector of a photon scattered from the direction $\vec{l}$ towards the observer makes an angle ϕ with the $\vec{OY}$ axis, so the rotation to the standard axes needs to be implemented (see, e.g. Chandrasekhar 1950).

The intensity ΔI_ν is equal to the product of the optical depth τ as seen from the point (X,Y,Z) in the direction $\vec{l}$ and a geometry-independent factor which is determined by whether the kinematic or thermal effect has introduced the local anisotropy. For the thermal effect

$$\Delta I_\nu(X,Y,Z,\theta,\phi) = \tau(X,Y,Z,\theta,\phi)\eta I_\nu f_{\rm T}(x), \quad (27)$$

where I_ν is the CMB spectral intensity, and

$$f_{\rm T}(x) = \frac{xe^x}{e^x-1}\left(x\frac{e^x+1}{e^x-1}-4\right) \quad (28)$$

(Sunyaev & Zel'dovich 1972). In the case of the kinematic effect,

$$\Delta I_\nu(X,Y,Z,\theta,\phi) = -\tau(X,Y,Z,\theta,\phi)(\vec{l}\vec{\beta})I_\nu f(x), \quad (29)$$

where $\vec{\beta} = \beta(\sin\alpha\cos\psi, \sin\alpha\cos\psi, \cos\alpha)$ is the peculiar velocity vector, and the frequency dependence for the kinematic effect f is the same as that for the polarization produced by the CMB quadrupole, given by formula (10). Now we proceed to some examples.

4.2.1 Homogeneous spherical cloud

$$\rho(r) = \begin{cases} \rho_0, & r<1; \\ 0, & r>1. \end{cases}$$

For the $\beta\tau^2$ effect the calculations in equations (25), (26) can be completed analytically, yielding:

$$Q'_\nu = \frac{1}{20}(X\cos\psi - Y\sin\psi)\sqrt{1-(X^2+Y^2)}\beta_t\tau_0^2 I_\nu f(x), \quad (30)$$

$$U'_\nu = \frac{1}{20}(X\sin\psi + Y\cos\psi)\sqrt{1-(X^2+Y^2)}\beta_t\tau_0^2 I_\nu f(x), \quad (31)$$

where we have introduced $\tau_0 = 2\sigma_{\rm T}\rho_0$, the central optical depth.

The derived result is identical to that of Sunyaev & Zel'dovich (1980). One important property of the effect described by relations (30) and (31) is that its amplitude $((Q^2+U^2)^{1/2})$ depends only on the projected distance r from the cluster center. The azimuthal angle determines only the direction of polarization; the sign of the effect is different in the leading and trailing parts of the cluster (with respect to the direction of motion), as shown in Fig. 2(b). The maximal polarization degree is reached at $r_{\max} = 1/\sqrt{2}$ and is equal to $0.025\beta_t\tau_0^2 f(x)$. In the Rayleigh-Jeans region, this is simply $0.025\beta_t\tau_0^2$. One should note that in this case, in contrast to the effect of the order of $\beta_t^2\tau$, there is no net polarization from the cluster.

For the $\eta\tau^2$ effect, the integration in formulae (25), (26) can be implemented numerically. The polarization direction depends on the frequency of measurement in this case. At low frequencies, the polarization is radially directed in the picture plane – see Fig. 2(c). At $x=3.83$, the thermal effect changes its sign and at frequencies higher than this critical value, the polarization vector is orthogonal to the radius-vector, as shown in Fig. 2(d). The maximal polarization degree of $0.014\eta\tau_0^2 f_{\rm T}(x)$ is reached at $r=0.85$. In the Rayleigh-Jeans spectral region, $P=0.028\eta\tau_0^2$. Again, like for the $\beta\tau^2$ effect, the angular-integrated polarization is zero.

4.2.2 Spherical cloud, King's density law

$\rho(r) = [1+(r/r_c)^2]^{-n}$.

Fig. 3 shows how the polarization degree depends on the angular distance (r/r_c) from the cluster center for two values of n: 1 and 2. The maximal polarization is reduced by a factor of ~ 2 compared to the case of a homogeneous sphere for a given central optical depth τ_0.

4.2.3 Ellipsoidal cloud, King's density law

It is known from observations that the shape of clusters of galaxies often significantly differs from a spherical one.

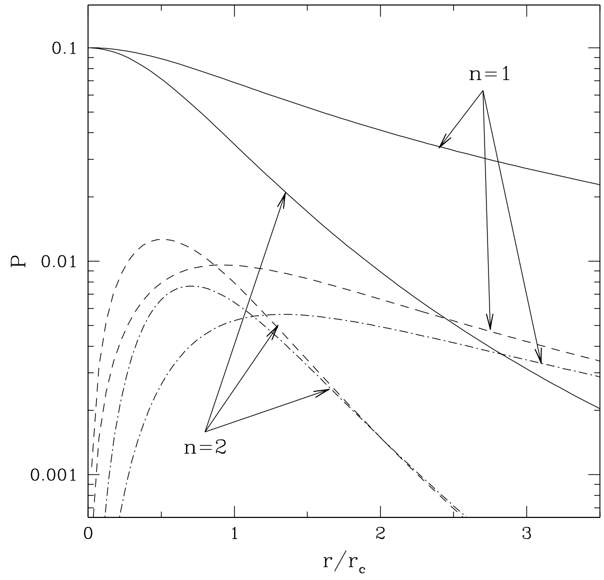

Figure 3. Various polarization effects as functions of projected distance from the cluster center, calculated for the spherical isothermal density model (for $n = 1$ and 2). Shown is a factor to be multiplied by: $\beta_t^2\tau_0$ (solid lines; for this effect as well as for the CMB quadrupole effect the angular dependence simply follows the angular dependence of the optical depth along the line of sight), $\beta_t\tau_0^2$ (dashed lines), and $(kT_e/m_ec^2)\tau_0^2$ (dash-dotted lines), where τ_0 is the central optical depth.

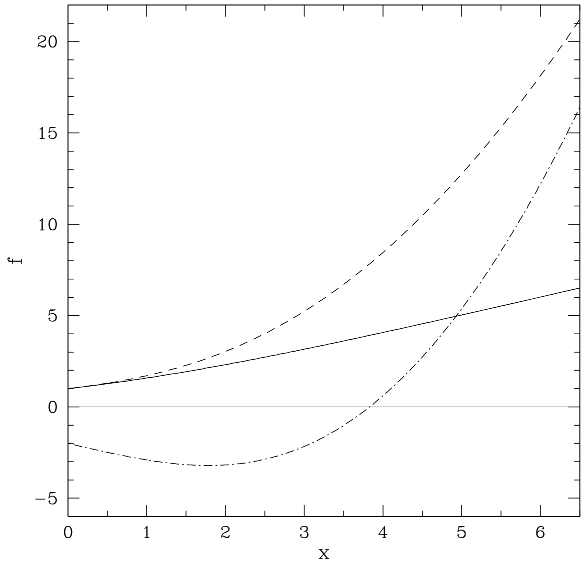

Figure 4. Various polarization effects as functions of frequency: the CMB quadrupole effect and the $\beta_t^2\tau$ effect (solid line), the $\beta_t\tau^2$ effect (dashed line), and the $(kT_e/m_ec^2)\tau^2$ effect (dash-dotted line). The latest effect changes its sign at $x = 3.83$.

The finite optical depth polarization effects will be modified notably in such situations. Let us consider an idealized model cluster which has a shape of the ellipsoid of revolution and whose density distribution is described by a modified isothermal law: $\rho(r) = [1 + (X/a)^2 + (Y^2 + Z^2)/b^2]^{-n}$. To make the situation more complete, we can rotate this ellipsoid around the $\vec{OY}$ axis. Examples of the resulting polarization pattern are presented in Fig. 2(e)–(g). The typical polarization degree is, in this case, of roughly the same magnitude as it was for the spherical cloud model, but its distribution in the picture plane can be absolutely different. In particular, generally, there is a polarized radiation in the direction of the cluster center – for example in Fig. 2(e) the degree of ellipsoidality (b/a) is only 0.8 but we see a maximum of polarization near the center, in sharp contrast to Fig. 2(c). Also important is that the net polarization from the cluster is no longer zero.

It is clear from the above that the angular distribution of the polarization caused by the finite depth effects for a given cluster will depend strongly on its shape and orientation, as well as on the distribution of gas within the cluster.

5 DISCUSSION

Microwave polarization measurements in directions of galaxy clusters provide a novel method for determining the quadrupole component in the CMB angular distribution, which does not require mapping of the whole sky, as is the case with the conventional method of measuring the CMB anisotropies. What is more important is that this method allows one to measure the CMB quadrupole component as would be seen by observers that are placed on distant clusters, including those at $z \sim 0.5$–3. This information, which is otherwise unaccessible, has significant implications for cosmology, which should raise interest of experimentators to microwave polarization measurements of distant clusters. Such measurements can at the same time provide another piece of information valuable for cosmology, namely that on the evolution of the peculiar velocities of clusters (Sunyaev & Zel'dovich 1981). The most serious concern is, of course, the small magnitude of the polarization induced by the CMB quadrupole, which is expected to be less than $\sim 0.1(\tau/0.02)$ μK. However, as we mentioned in Section 3, one can overcome the detector sensitivity limit by probing a large number of clusters.

Another problem is the presence of several other polarization effects connected with clusters of galaxies. These effects, which are interesting in their own right because they could, in principle, provide us such important information as on cluster tangential velocities and the distribution of intracluster gas, can produce a polarization comparable in size with that due to the CMB quadrupole, and will thus be a source of significant noise for observations aiming at the detection of the quadrupole-induced signal. Fortunately, all of these effects have a tendency to vanish in the course of averaging over a large cluster sample. Let us see how significantly the different polarization mechanisms could contribute to an individual measurement.

The polarizations due to the three basic effects are of

© 0000 RAS, MNRAS **000**, 000–000

the order of $0.1\beta_t^2\tau$, $0.01\beta_t\tau^2$ and $0.01\eta\tau^2$ in the Rayleigh-Jeans spectral region (the coefficients for the last two effects are model-dependent, but typically do not differ much from the quoted values). The first effect becomes equal to the CMB quadrupole polarization effect at its maximum for the tangential velocity ~ 1300 km/s (as implied by the COBE data). This value is considerably higher than the average peculiar velocity expected for clusters of galaxies (see, e.g. Bahcall & Oh 1996). Moreover, the sky-average of the polarization signal due to the CMB quadrupole is $\sim 60\%$ of the maximum value, whereas the velocity effect is proportional to the square of β_t, and therefore for typical values, $\beta_t \sim 400$ km/s, the polarization produced by the CMB quadrupole should be several times stronger in the Rayleigh-Jeans region of the CMB spectrum. Among the considered effects, only the $0.01\eta\tau^2$ polarization might compete with the quadrupole-induced polarization for rich clusters.

The above values were calculated for the Rayleigh-Jeans spectral region, which corresponds to centimeter and millimeter wavelengths. However, the polarization degree will strongly depend on frequency if one performs measurements in the short millimeter and, especially, in the submillimeter band. The frequency dependencies for the different effects are shown in Fig. 4. Note that the polarization due to the CMB quadrupole has the same frequency dependence as the $\beta_t\tau^2$ polarization, both growing linearly ($\sim x$) in the Wien part of the spectrum. The other two effects rise more steeply, $\sim x^2$, in the Wien region. The different frequency behaviours provide us an opportunity to separate the signals of different nature by carrying out multi-band observations. On the other hand, it is clear that there is more hope to detect the polarization due to the CMB quadrupole in the Rayleigh-Jeans region, where its contribution is relatively more significant.

The effects being discussed also depend in different ways on the projected angular distance from the cluster center. The CMB quadrupole effect and the $\beta_t^2\tau$ effect are proportional to the optical depth along a given line of sight, and therefore both lead to a finite polarization of the signal integrated over the picture plane. The other two effects have a tendency to vanish in the net signal. This fact significantly enhances our chances to determine both the CMB quadrupole and the tangential velocities of clusters by means of polarization measurements – one just has to accumulate the microwave signal from the whole cluster (or at least from an area which is symmetric around its center). Furthermore, the $\beta_t^2\tau$ polarization will vanish upon averaging over a large set of clusters, unless the directions of their tangential motions are correlated, enabling the extraction of the pure quadrupole-induced signal. Fig. 5 demonstrates the complexity of the overall problem. It shows how the polarization pattern shaped purely by the CMB quadrupole anisotropy will be modified by the other polarization effects and undergo further changes if one tunes to a different measurement frequency.

It is worth noting that other polarization effects, apart from those discussed in this paper, may appear strong under some circumstances. For example, the signal from a cluster can be polarized if there is a strong compact source of unpolarized radio emission inside the cluster (Sunyaev & Zel'dovich 1980; Sunyaev 1982). The polarization pattern in this case will be similar to that produced by the $\eta\tau^2$ effect – see Fig. 2(d). Of course, the frequency dependence in this case, which should be power-law-like, will markedly distinguish itself. Another way to give rise to polarization is through gravitational mechanisms (Gibilisco 1997), which we already mentioned above. Finally, there is a polarization which is intrinsic to the CMB. This polarization signal, which together with the intensity fluctuations has been brought to us largely from the epoch of decoupling but may also bear imprints from later epochs, is expected to be very small at sub-arcminute scales which correspond to the typical dimensions of cluster cores (see, e.g. Seljak & Zaldarriaga 1998; White 1998). It should also be noted that the typical Faraday rotation measures of galaxy clusters are too small to produce a significant depolarization of the discussed effects for wavelengths below ~ 10 cm, i.e. in the domain of interest to us (Lawler & Dennison 1982; Sarazin 1988).

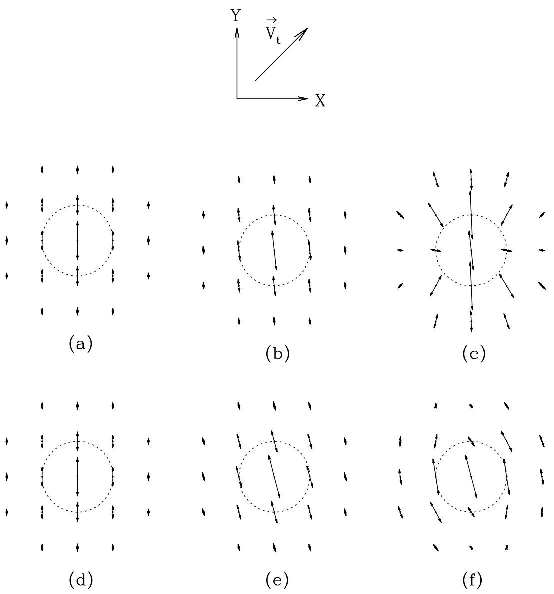

Figure 5. Combined effect of the CMB quadrupole and other mechanisms on the polarization from a cluster which is located in the direction of the maximum of the quadrupole-induced polarization, has a transverse velocity of 600 km/s ($\beta_t = 0.02$), central optical depth $\tau = 0.01$ and gas temperature 5 keV ($kT_e/m_ec^2 = 0.01$). The density distribution is assumed to be $(1 + (r/r_c)^2)^{-3/2}$, where r_c is the core-radius which defines the size of the circle shown on each panel. (a) Only the quadrupole-induced polarization. (b) The $\beta_t^2\tau$ effect has been added. (c) The effect $(kT_e/m_ec^2)\tau^2$ has been added. Cases (a)–(c) are for the Rayleigh-Jeans spectral region. (d)–(f) The same as (a)–(c) but for the frequency $x = 5$.

REFERENCES

Audit E., Simmons J. F. L., 1999, MNRAS, 305, L27
Bahcall N. A., Oh S. P., 1996, ApJ, 462, L49
Bennett C. L. et al., 1996, ApJ, 464, L1
Chandrasekhar S., 1950, Radiative Transfer. Dover, New York

Cortiglioni S. et al., 1999, in Proc. 3K Cosmology Rome 1998, AIP Conference Proc., in press; astro-ph/9901362
De Zotti. G. et al. 1999, in Proc. 3K Cosmology Rome 1998, AIP Conference Proc., in press; astro-ph/9902103
Gibilisco M., 1997, ApSS, 249, 189
Hansen F. K., Lilje P.B., 1999, MNRAS, 306, 153
Itoh N., Nozawa S., Kohyama Y., 1998, astro-ph/9812376
Kamionkowski M., Loeb A., 1997, Phys. Rev. D., 56, 4511
Keating B., Timble P., Polnarev A., Steinberger J., 1998, ApJ, 495, 580
Kogut A., Banday A. J., Bennett C. L., Gorski K. M., Hinshaw G., Smoot G. F., Wright E.L., 1996, ApJ, 464, L5
Lawler J. M., Dennison B., 1982, ApJ, 252, 81
Sarazin C.L., 1988, X-ray emission from clusters of galaxies. Cambridge University Press, Cambridge
Seljak U., Zaldarriaga M., 1998, in Fundamental Parameters in Cosmology, Proc. XXXIIIrd Rencontres de Moriond, in press; astro-ph/9805010
Sunyaev R. A., 1982, Astronomy Letters, 8, 175
Sunyaev R. A., Zel'dovich Y. B., 1972, Comments Astrophys. Space Phys., 4, 173
Sunyaev R. A., Zel'dovich Y. B., 1980, MNRAS, 190, 413
Sunyaev R. A., Zel'dovich Y.B., 1981, in Sunyaev R., ed, Soviet Scientific Reviews Sect. E: Astrophysics and Space Physics Rev., vol. 1. Harwood Academic Publishers, New York, p. 1
White M., 1998, in Proc. Evolution of Large Scale Structure, Garching 1998, in press; astro-ph/9810506
Zel'dovich Y. B., Sunyaev R.A., 1980, Astronomy Letters, 6, 285